

Aluminothermic Reduction of CeO₂: Mechanism of an economical route to Aluminum-Cerium Alloys

Alfred Amon,^a Emily E. Moore,^a Hunter B. Henderson,^a Jibril Shittu,^a Martin Kunz,^b Shane Kastamo,^c Nikolai Huotari,^c Adam Loukus,^c Ryan Ott,^d David Weiss,^c and Scott K. McCall^a

^aLawrence Livermore National Laboratory, 7000 East Ave, Livermore, CA 94550, USA

^bLawrence Berkeley National Laboratory 1 Cyclotron Rd, Berkeley, CA 94720, USA

^cLoukus Technologies Inc., 58390 Centennial Number 6 Road, Calumet, MI 49913, USA

^dAmes National Laboratory, 2415 Pammel Dr., Ames, IA, 50011, USA

Correspondence

Email: moore255@llnl.gov and amon1@llnl.gov

Methods

Samples for reduction experiments were prepared by combining Al powder (99 %, 17-30 μm) and CeO_2 powder (99 %, < 75 μm , as received) in a ceramic mortar with a 7:1 molar ratio under argon atmosphere and pressing the powder mixture to tablets using a hydraulic press (750 MPa). Differential Scanning Calorimetry data were collected on a TA SDT-650 under argon atmosphere. After rapid heating (50 K min^{-1}), samples (35-40 mg each) were kept at the isothermal hold temperature until reaction completion. Calibration at isothermal conditions was not reliable enough to quantify the absolute heat evolved during the process. Laboratory PXRD data were collected on powdered samples with a Bruker D8 (Cu-K α radiation). Synchrotron diffraction data were collected on beamline 12.2.2 at the Advanced Light Source at Lawrence Berkeley National Lab.^[32] The samples, loaded in 0.7 mm diameter fused silica capillaries, were heated at 10 $^\circ\text{C s}^{-1}$ to the target temperature using the beamlines IR lamp heater set-up^[33] while under constant Ar flow^[34]. Cooling rates were 5 $^\circ\text{C s}^{-1}$. Two seconds exposure diffraction patterns were collected continuously using a Dectris Pilatus3 S 1M detector. Beamline and detector geometry were calibrated using the diffraction pattern of a NIST-SRM 674b CeO_2 . X-ray energy (set to 25 keV) and sample to detector distance were refined to 25.11 keV and 213.50 mm, respectively. The furnace's temperature was calibrated using both an S-type (Omega P10R-005) thermocouple as well as a Pt diffraction calibrant and subsequently controlled through an S-type thermocouple. Overall compositions of synchrotron diffraction samples were estimated by Rietveld refinement on first frame data before heating started. Samples were heated at 300 K min^{-1} and kept at the respective hold temperature until reaction completion (20 to 80 min). The furnace temperature was calibrated with a thermocouple at the sample position beforehand. Data reduction and Rietveld refinements were done using the DAWN Scientific^[35,36] and GSAS2^[37] software packages, respectively. After data reduction, the phase evolution was monitored by peak integration of selected peaks (Al (hkl = 111), CeO_2 (111), $\text{Ce}_3\text{O}_{5+x}$ (211), Ce_2O_3 (010), CeAlO_3 (100), $\text{Ce}_3\text{Al}_{11}$ (002)). Curves in Figures 3 and S8 were smoothed with a 10-point moving average filter, as capillary movement, and rotation of crystallites in the beam led to rapid fluctuations in peak intensities. The small number of crystallites of the product phases in the sample and concomitant strong preferred orientation effects on the peak intensities obstructed a reliable quantitative analysis for the reacted synchrotron samples. Crystal structure data for Rietveld refinement were obtained from the ICSD data base for the phases: Al (space group: Fm-3m, ICSD entry code:

43423), Al₂O₃ (R-3c, 9770), CeAlO₃ (Pm-3m, 245565), Ce₂O₃ (P-3m, 100204), Ce₃O_{5+x} (Ia-3, 88752), CeO₂ (Fm-3m, 24887), Ce₃Al₁₁ (Immm, 1614983). Parameters regarding peak shape, instrumental contributions and lattice parameters were refined but atomic positions, atomic displacement and site occupation were kept at given values. Electron micrographs and spectroscopy data were collected on polished sample pieces after DSC using a ThermoFisher Apreo 2 (20 kV beam voltage) with an Octane Elite EDS detector.

Equilibrium calculations were performed using the CALPHAD (CALculation of PHase Diagrams) method that is based on mathematical models that use adjustable parameters to describe a set of self-consistent Gibbs energy functions.^[38–40] A thermodynamic database was developed based on the binary descriptions for the Al-Ce,^[41] Al-O^[42] and Ce-O^[27] systems, where the oxide data is readily available on the TAF-ID.^[43] A ternary phase exists with the composition AlCeO₃, that is stable until temperature 2030°C.^[44] This phase has not been previously assessed using the CALPHAD method and was included in this database. The binary systems were used in the extrapolation of the ternary phase, where a Neumann-Kopp^[45] type algebraic sum of the oxides in their standard states (i.e. Al₂O₃ and Ce₂O₃) was used as initial values for the Gibbs energy expression and adjusted to reflect stability with respect to the oxide binary phases. The formation energy of the AlCeO₃ compound was also used as a reference when stabilizing the ternary phase and is calculated to be 1764 kJ mol⁻¹ compared to the value from Kubaschewski et al.^[46] A ternary phase diagram is calculated at 950 °C in Figure 4A, whereas the stable phases along the CeO₂ — Al join are calculated as a function of Al-content in Figure 4B.

Table S1. Relative phase amounts from full pattern Rietveld refinement for the sample after DSC measurement at 850 °C, 900 °C and 950 °C.

Phase	Mole fraction 850 °C	Mole fraction 900 °C	Mole fraction 950 °C
CeO ₂	0.05	< 0.01	0
Al	0.79	0.59	0.62
3x Ce ₃ Al ₁₁	0.09	0.19	0.18
Al ₂ O ₃	0.06	0.21	0.18
CeAlO ₃	0.01	< 0.01	0.02

Table S2. EDS analysis results for sample after DSC at 950 °C, points from Figure S4.

Point	Al at %	Ce at %	O at. %
1	99.9	0.1	
2	47.6	18.9	33.8
3	31.5	0.6	67.9
4	80.2	19.8	
5	99.9	0.1	
6	98.8	1.2	
7	14.2	31.5	54.3
8	5.9	72.3	21.8
9	58.2	3.8	38.0

Table S3. EDS analysis results for sample after DSC at 850 °C, points from Figure S6.

Point	Al at %	Ce at %	O at. %
1	23.0	77.0	
2	21.8	78.2	
3	21.2	78.8	
4	17.7	82.3	
5	99.9	0.1	
6	98.8	1.2	
7	14.2	31.5	54.3
8	5.9	72.3	21.8
9	58.2	3.8	38.0

Table S4: Estimated relative phase fractions of selected crystalline phases at different times during the in-situ synchrotron experiments, determined from Rietveld refinement. Normalized by cerium content.

Phase	850 °C						900 °C			950 °C				
	0 s	154 s	249 s	649 s	1149 s	2057 s	0 s	88 s	354 s	0 s	72 s	100 s	200 s	250 s
CeO _{2-x}	0.12	0	0	0	0.33	0.32	0.7	0	0	0.07	0.16	0.01	0	0
Al (fcc)	0.99	0	0	0	0.64	0.66	0.93	0	0	0.93	0	0	0	0
½ x Ce ₂ O ₃	0	0.18	0.39	0.46	0	0	0	0.22	0.09	0	0.12	0.38	0.34	0.07
CeAlO ₃	0	0.01	0.01	0.01	0	0	0	0.03	0.91	0	0.01	0.45	0.66	0.93
1/3 x Ce ₃ O _{5+x}	0	0.81	0.60	0.53	0	0	0	0.75	0	0	0.71	0.16	0	0
1/3 x Ce ₃ Al ₁₁	0	0	0	0	0.03	0.02	0	--	--	0	0	0	0	0

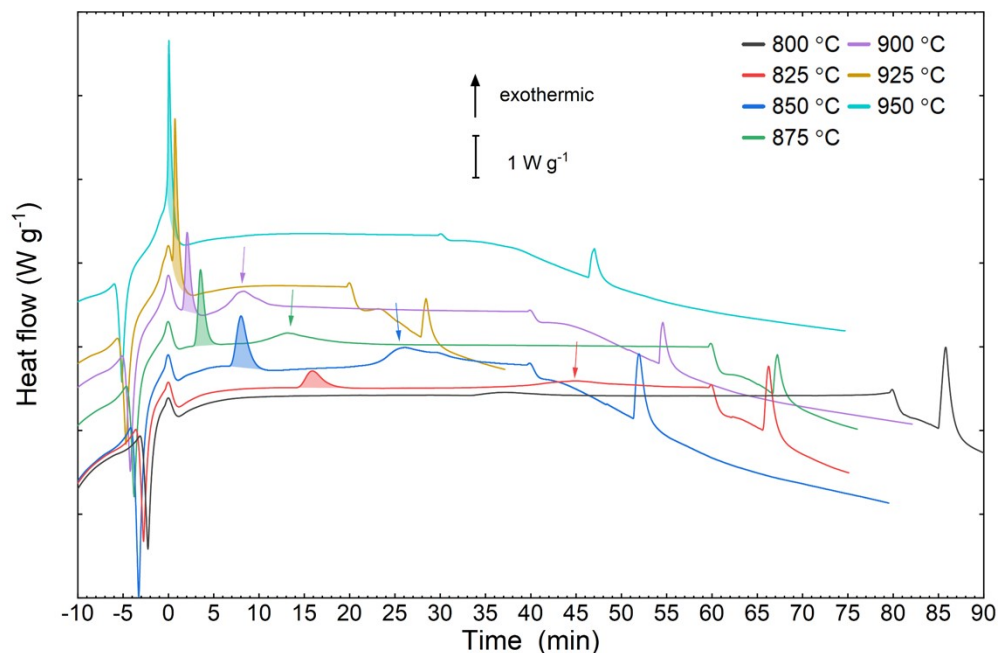


Figure S1. Complete DSC curves of data segments shown in Figure 1. $t = 0$ min corresponds to the beginning of the isothermal hold time, which varied in length depending on the temperature. Melting and solidification of aluminum manifests as sharp endo- and exothermal peaks before and after the isothermal segment, respectively. Curves are shifted vertically for clarity. Arrows highlight the second delayed thermal effects observed.

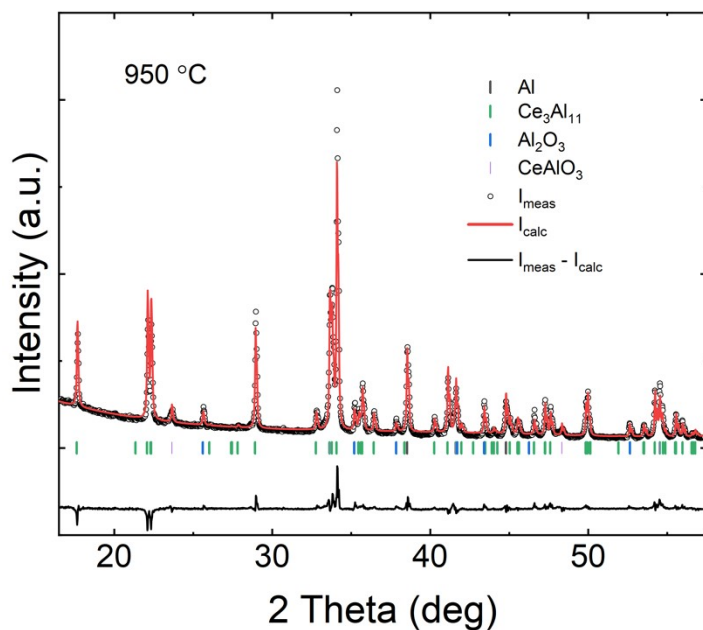


Fig. S2 Laboratory PXRD pattern for Al + CeO₂ reacted at 950 °C (circles) with calculated profile from Rietveld refinement (red line) and difference plot (black line). Peak positions for phases are indicated. $R_p = 9.2\%$, $wR_p = 11.9\%$, $R_{exp} = 2.6\%$, Phases: Al ($a = 4.0444(2)$ Å), CeAlO₃ ($a = 3.7636(4)$ Å), Al₂O₃ ($a = 4.753(1)$ Å, $c = 12.982(2)$ Å), Ce₂Al₁₁ ($a = 4.3883(1)$ Å, $b = 10.0523(4)$ Å, $c = 13.0093(5)$ Å). Phase amounts in Table S1.

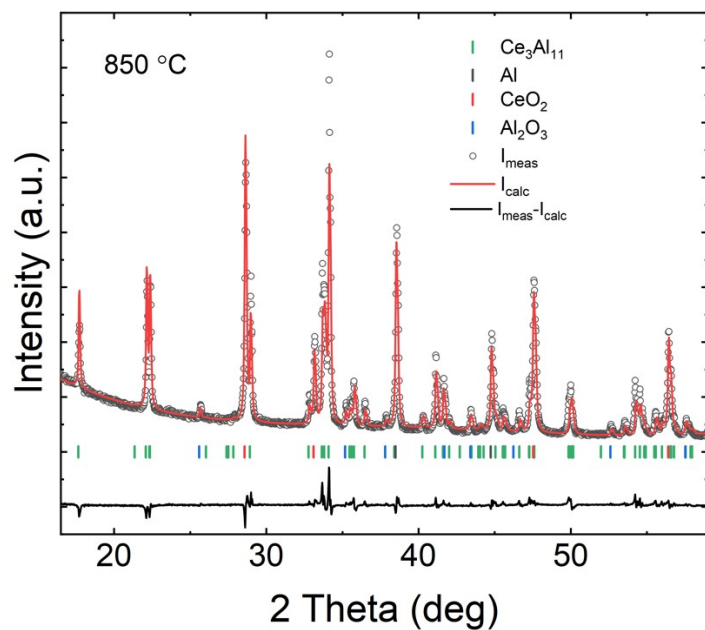


Fig. S3 Laboratory PXRD pattern for Al + CeO₂ reacted at 850 °C (circles) with calculated profile from Rietveld refinement (red line) and difference plot (black line). Peak positions for phases are indicated. $R_p = 8.3\%$, $wR_p = 11.8\%$, $R_{exp} = 2.5\%$, Phases: Al ($a = 4.0450(2)$ Å), CeO₂ ($a = 5.4054(2)$ Å), Al₂O₃ ($a = 4.753(3)$ Å, $c = 12.984(4)$ Å), Ce₃Al₁₁ ($a = 4.3879(2)$ Å, $b = 10.0513(6)$ Å, $c = 13.0079(7)$ Å). Phase amounts in Table S1.

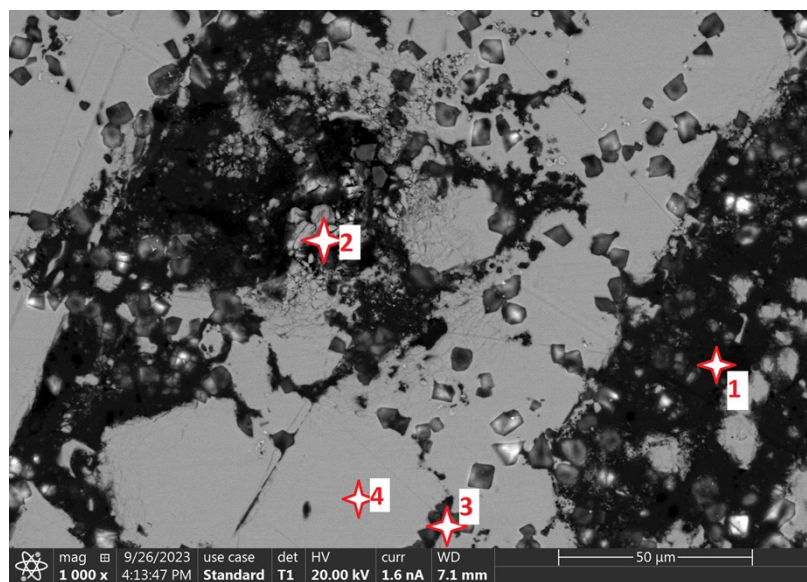


Figure S4: Locations of EDS point measurements on sample after DSC at 950 °C (cf. Table S2).

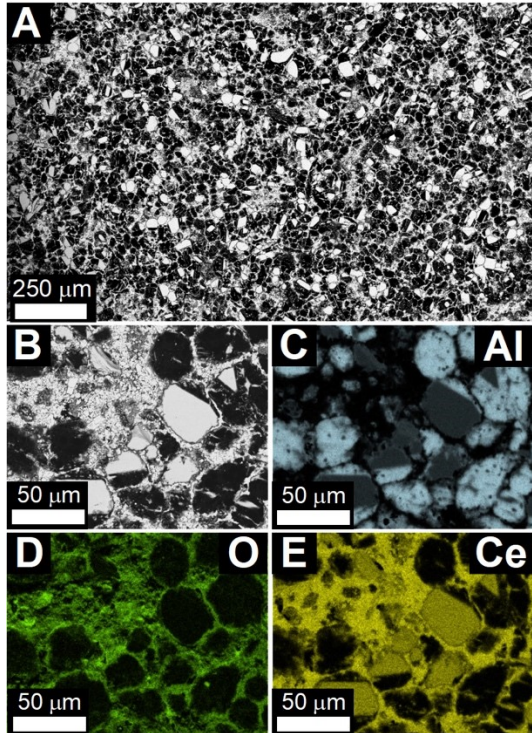


Fig. S5: Scanning electron microscopy on Al-CeO₂ sample after DSC reacted at 850 °C. A: Secondary electron image showing a mixture of Ce₃Al₁₁ grains (bright phase), Al dendrites (dark) and unreacted oxides. B: High-magnification backscatter-electron. C-E: EDS elemental mapping of Al, O, and Ce distribution in the microstructure.

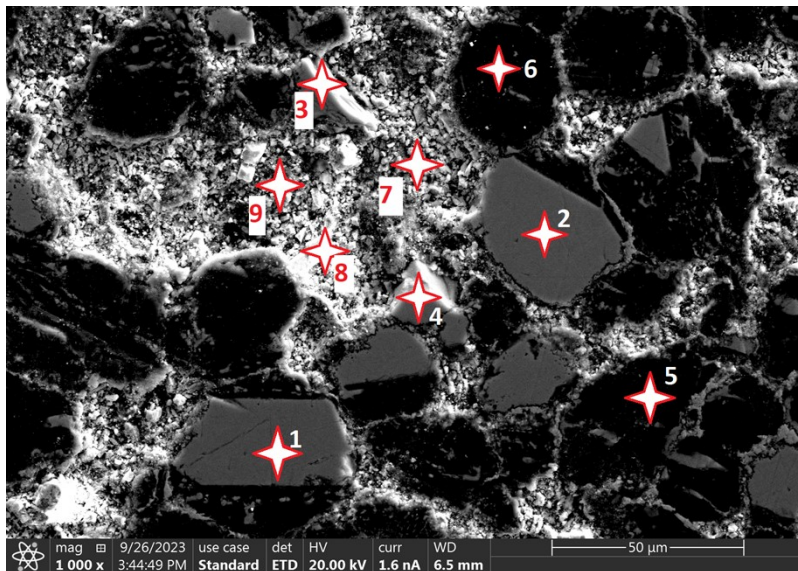


Figure S 6: Locations of EDS point measurements on sample after DSC at 850 °C (cf. Table S3).

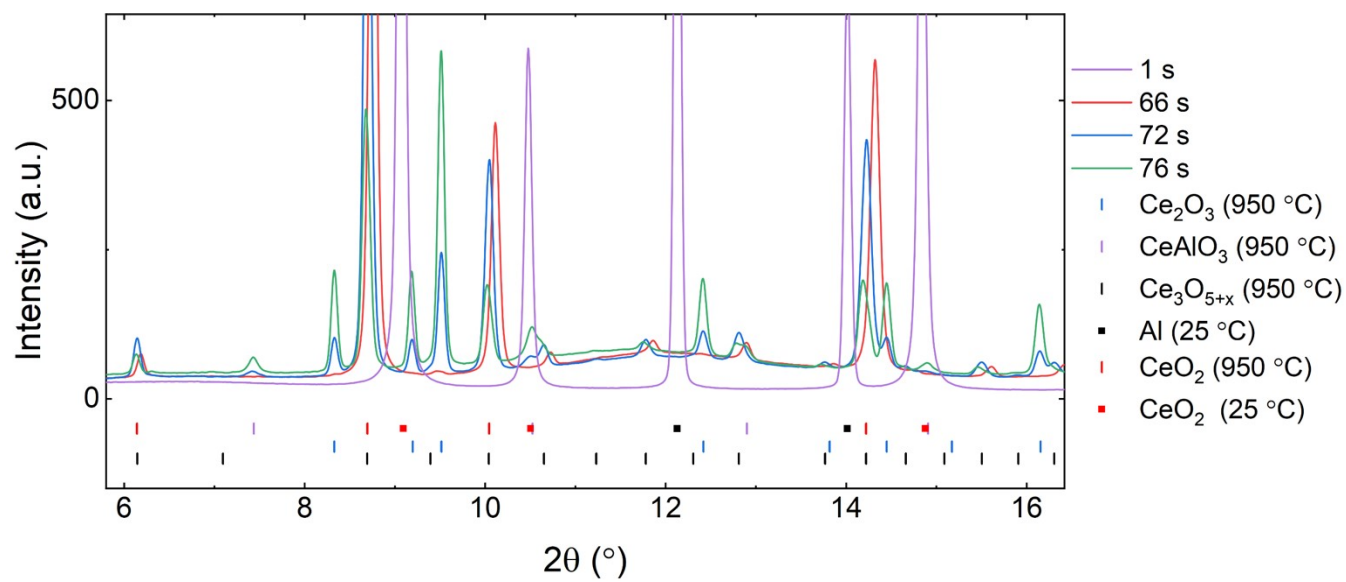


Figure S7. Selected frames from time-resolved synchrotron diffraction results for the reaction of Al with CeO_2 at 950°C . Calculated peak positions are given as tick marks (for 950°C) and squares (for 25°C).

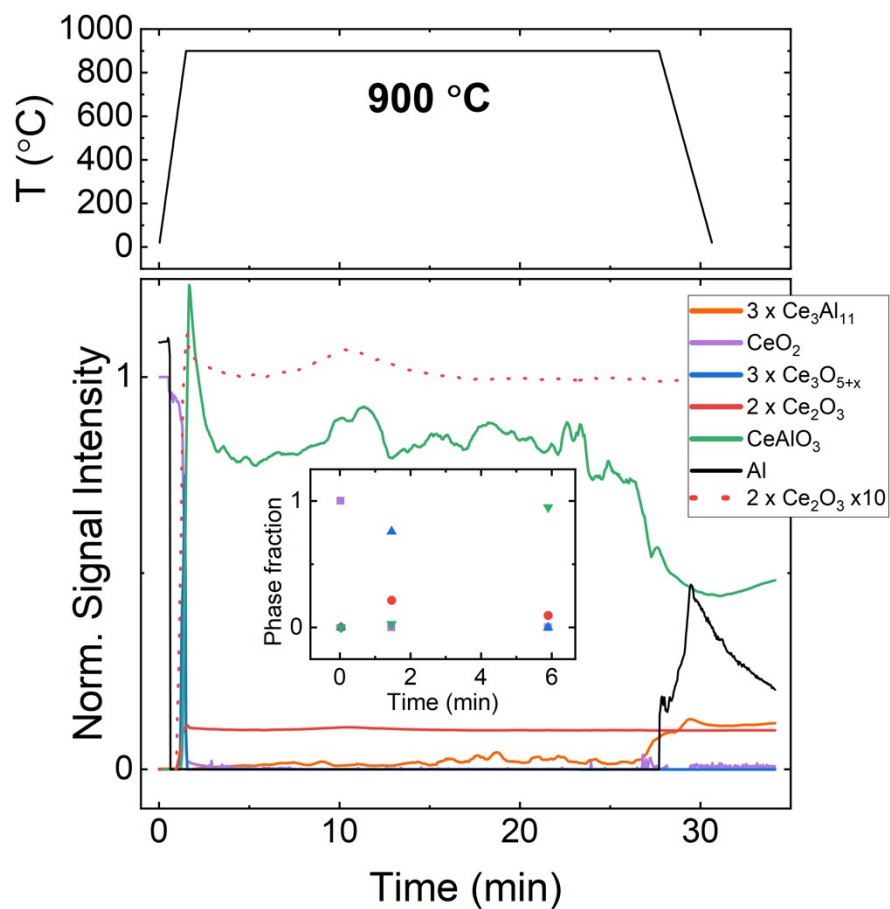


Figure S8. Time-resolved synchrotron diffraction results for the reaction of Al with CeO₂ at 900 °C, together with temperature program. Curves for respective phases are normalized using results from Rietveld refinements to approximately reflect the evolution of relative phase amounts over time. Inset: Relative amounts of Ce-oxide phases determined at selected times, normalized by Ce content.